

# Microwave-resonance-induced magnetooscillations and vanishing resistance states in multisubband two-dimensional electron systems

Yu.P. Monarkha<sup>1</sup>

<sup>1</sup>*Institute for Low Temperature Physics and Engineering, 47 Lenin Avenue, 61103 Kharkov, Ukraine*

The dc magnetoconductivity of the multisubband two-dimensional electron system formed on the liquid helium surface in the presence of resonant microwave irradiation is described, and a new mechanism of the negative linear response conductivity is studied using the self-consistent Born approximation. Two kinds of scatterers (vapor atoms and capillary wave quanta) are considered. Besides a conductivity modulation expected near the points, where the excitation frequency for inter-subband transitions is commensurate with the cyclotron frequency, a sign-changing correction to the linear conductivity is shown to appear for usual quasi-elastic inter-subband scattering, if the collision broadening of Landau levels is much smaller than thermal energy. The decay heating of the electron system near the commensurability points leads to magnetooscillations of electron temperature, which are shown to increase the importance of the sign-changing correction. The line-shape of magnetoconductivity oscillations calculated for wide ranges of temperature and magnetic field is in a good accordance with experimental observations.

PACS numbers: 73.40.-c, 73.20.-r, 73.25.+i, 78.70.Gq

## I. INTRODUCTION

The discovery of novel microwave-induced oscillations of magnetoresistivity<sup>1</sup> as a function of the magnetic field  $B$  and so-called zero-resistance states (ZRS)<sup>2,3</sup> has sparked a large interest in quantum magnetotransport of two-dimensional (2D) electron systems exposed to microwave (MW) radiation. The  $1/B$ -periodic oscillations were observed for quite arbitrary MW frequencies  $\omega$  larger than the cyclotron frequency  $\omega_c$ . The period of these oscillations is governed by the ratio  $\omega/\omega_c$ . ZRS appear in ultrahigh-mobility GaAs/AlGaAs heterostructures as a result of evolution of the minima of the oscillations with an increase in radiation power.

Recently, MW-induced magnetooscillations and vanishing of the magnetoconductance  $\sigma_{xx}$  were observed in the nondegenerate multisubband 2D electron system formed on the liquid helium surface<sup>4,5</sup>. These oscillations have many striking similarities with those observed in semiconductor systems: they are  $1/B$ -periodic, governed by the ratio  $\omega/\omega_c$ , and their minima eventually evolve in zero magnetoconductance states nearly at the same values of  $\omega/\omega_c$ . The important distinction of these new oscillations is that they are observed only for a MW frequency fixed to the resonance condition for excitation of the second surface subband:  $\hbar\omega = \Delta_{2,1}$  (here  $\Delta_{l,l'} = \Delta_l - \Delta_{l'}$ , and  $\Delta_l$  describes the energy spectrum of surface electron states,  $l = 1, 2, \dots$ ).

The ZRS observed in semiconductor systems are shown<sup>6</sup> to be understood as a direct consequence of the negative photoconductivity  $\sigma_{xx} < 0$  which can appear with an increase in the amplitude of conductivity oscillations. Regarding the microscopic origin of the oscillations, the most frequently studied mechanism is based on photon-induced impurity scattering within the ground subband, when an electron simultaneously is scattered off impurities and absorb or emit microwave quanta<sup>7,8</sup>.

This kind of scattering is accompanied by an electron displacement along the applied dc-electric field whose sign depends on the sign of  $\omega_c(n - n') + \omega$  (here  $n = 0, 1, \dots$ ). Therefore, sometimes this mechanism is termed the "displacement" mechanism. A different mechanism, called the "inelastic" mechanism<sup>9</sup>, explains conductivity oscillations as a result of oscillatory changes of the isotropic part of the in-plane electron distribution function.

Both microscopic mechanisms of the negative conductivity proposed for semiconductor systems cannot be applied for explanation of similar effects observed in the system of surface electrons (SEs) on liquid helium, because the MW frequency considered in these theories has no relation to inter-subband excitation frequencies  $\Delta_{l,l'}/\hbar \equiv \omega_{l,l'}$ . Recently, a new mechanism of negative momentum dissipation relevant to experiments with SEs on liquid helium was briefly reported<sup>10</sup>. It cannot be attributed to "displacement" or "inelastic" mechanisms. In this theory, the origin of magnetooscillations and negative dissipation is an additional filling of the second surface subband induced by MW irradiation under the resonance condition ( $\hbar\omega = \Delta_{2,1}$ ), which triggers quasi-elastic inter-subband electron scattering. The ordinary inter-subband scattering, which does not involve photon quanta, is accompanied by electron displacements whose sign depends on the sign of  $\omega_c(n - n') + \omega_{2,1}$ . Usually, this scattering does not lead to any negative contribution to  $\sigma_{xx}$ . A correction to  $\sigma_{xx}$  proportional to  $\omega_c(n - n') + \omega_{2,1}$  was shown to appear only if  $N_2 > N_1 e^{-\Delta_{2,1}/T_e}$ , where  $N_l$  is the number of electrons at the corresponding subband, and  $T_e$  is the electron temperature. It is important that this correction is also proportional to a large parameter equal to the ratio of  $T_e$  to the collision broadening of Landau levels.

In this work, we perform a systematic theoretical study of negative dissipation phenomena in a multisubband 2D electron system caused by non-equilibrium filling of excited subbands. The magnetotransport theory<sup>10</sup> is gener-

alized in order to include electron scattering by capillary wave quanta (rippions) which limits SE mobility in experiments<sup>5</sup>, where vanishing magnetoconductivity  $\sigma_{xx}$  is observed. In order to understand the importance of MW heating at the vicinity of commensurability points, electron energy relaxation is analyzed. A sign-changing correction to the energy relaxation rate similar to the sign-changing correction to the momentum relaxation rate is found for non-equilibrium filling of excited subbands.

## II. GENERAL DEFINITIONS

Consider a multisubband 2D electron system under magnetic field applied perpendicular. The electron energy spectrum is described by  $\Delta_l + \varepsilon_n$ , where  $\varepsilon_n = \hbar\omega_c(n+1)$  represents Landau levels ( $n = 0, 1, 2, \dots$ ). For SEs on liquid helium (for review see Ref. 11) under a weak holding electric field ( $E_\perp \rightarrow 0$ ),  $\Delta_l \simeq -E_R/l^2$ , where  $E_R$  is the effective Rydberg energy of SE states,

$$E_R = \frac{\hbar^2}{2m_e a_B^2}, \quad a_B = \frac{\hbar^2}{m_e \Lambda}, \quad \Lambda = \frac{e^2(\epsilon - 1)}{4(\epsilon + 1)}, \quad (1)$$

$a_B$  is the effective Bohr radius,  $m_e$  is the electron mass, and  $\epsilon$  is the dielectric constant of liquid helium. The excitation energy  $\Delta_{2,1}$  is about 6 K (liquid <sup>4</sup>He) or 3.2 K (liquid <sup>3</sup>He). It increases with the holding electric field  $E_\perp$ , which allows also to tune  $\Delta_{2,1}$  in resonance with the MW frequency.

Under typical experimental conditions, the electron-electron collision rate  $\nu_{e-e}$  of SEs is much higher than the energy and momentum relaxation rates. Therefore, the electron distribution as a function of the in-plane energy  $\varepsilon$  can be characterized by the effective electron temperature,

$$f_l(\varepsilon) = N_l \frac{2\pi l_B^2}{AZ_\parallel} e^{-\varepsilon/T_e}, \quad (2)$$

where  $l_B^2 = \hbar c/eB$ , and  $A$  is the surface area. According to the normalization condition  $\int f_l(\varepsilon) D_l(\varepsilon) d\varepsilon = N_l$  [here  $D_l(\varepsilon)$  is the density-of-state function for the corresponding subband],  $Z_\parallel = \sum_n e^{-\varepsilon_n/T_e}$ .

The approach reported here will be formulated in a quite general way to be applicable for any weak quasi-elastic scattering. As important examples, we shall consider interactions which are well established for SEs on liquid helium. Vapor atoms are described by a free-particle energy spectrum  $\varepsilon_{\mathbf{K}}^{(a)} = \hbar^2 K^2/2M$  with  $M \gg m_e$ . For electron interaction with vapor atoms, it is conventional to adopt the effective potential approximation

$$H_{int}^{(a)} = V^{(a)} \sum_e \sum_a \delta(\mathbf{R}_e - \mathbf{R}_a), \quad (3)$$

where  $V^{(a)}$  is proportional to the electron-atom scattering length<sup>12</sup>. Ripplons represent a sort of 2D phonons,

and the electron-riplon interaction Hamiltonian is usually written as

$$H_{int}^{(r)} = \frac{1}{\sqrt{A}} \sum_e \sum_{\mathbf{q}} U_q(z_e) Q_q \left( b_{\mathbf{q}} + b_{-\mathbf{q}}^\dagger \right) e^{i\mathbf{q}\cdot\mathbf{r}_e}, \quad (4)$$

where  $Q_q = \sqrt{\hbar q/2\rho\omega_q}$ ,  $\omega_q \simeq \sqrt{\alpha/\rho} q^{3/2}$  is the ripplon spectrum,  $\mathbf{R}_e = \{z_e, \mathbf{r}_e\}$ ,  $\hbar\mathbf{q}$  is the ripplon momentum,  $b_{-\mathbf{q}}^\dagger$  and  $b_{\mathbf{q}}$  are the creation and destruction operators, and  $U_q(z_e)$  is the electron-riplon coupling<sup>11</sup> which has a complicated dependence on  $q$ .

For both kinds of SE scattering, the energy exchange at a collision is extremely small, which allows to consider scattering events as quasi-elastic processes. In the case of vapor atoms, it is so because  $M \gg m_e$ . One-riplon scattering processes are quasi-elastic ( $\hbar\omega_q \ll T$ ) because the wave-vector of a ripplon involved is usually restricted by the condition  $ql_B \lesssim 1$ .

For quasi-elastic processes in a 2D electron system under magnetic field, probabilities of electron scattering are usually found in the self-consistent Born approximation (SCBA)<sup>13</sup>. Following Ref. 14, we shall express the scattering probabilities in terms of the level densities at the initial and the final states. Then, Landau level densities will be broadened according to the SCBA<sup>13</sup> or to the cumulant expansion method<sup>15</sup>,

$$D_l(\varepsilon) = -\frac{A}{2\pi^2 l_B^2 \hbar} \sum_n \text{Im} G_{l,n}(\varepsilon), \quad (5)$$

where  $G_{l,n}(\varepsilon)$  is the single-electron Green's function. The later method is a bit more convenient for analytical evaluations because it results in a Gaussian shape of level densities

$$-\text{Im} G_{l,n}(\varepsilon) = \frac{\sqrt{2\pi}\hbar}{\Gamma_{l,n}} \exp\left[-\frac{2(\varepsilon - \varepsilon_n)^2}{\Gamma_{l,n}^2}\right]. \quad (6)$$

Here  $\Gamma_{l,n}$  coincides with the broadening of Landau levels given in the SCBA. For different scattering regimes of SEs, equations for  $\Gamma_{l,n}$  are given in Ref. 11. We shall also take into account an additional increase in  $\Gamma_{2,n}$  due to inter-subband scattering.

Effects considered in this work are important only under the condition  $\Gamma_{l,n} \ll T$  which is fulfilled for SEs on liquid helium. Therefore, we shall disregard small corrections to  $Z_\parallel$  caused by collision broadening because they are proportional to  $\Gamma_{l,n}^2/8T_e^2$ . In other equations, sometimes we shall keep terms proportional to  $\Gamma_{l,n}/T_e$ , if they provide important physical properties.

Average scattering probabilities of SEs on liquid helium and even the effective collision frequency  $\nu_{\text{eff}}$  can be expressed in terms of the dynamical structure factor (DSF) of the 2D electron liquid<sup>11</sup>  $S(q, \omega)$ . This procedure somehow reminds the theory of thermal neutron (or X-ray) scattering by solids, where the scattering cross-section is expressed as an integral form of a DSF. Without MW irradiation, most of unusual properties of the

quantum magnetotransport of SEs on liquid helium are well described by the equilibrium DSF of the 2D electron liquid<sup>11,16</sup>. A multisubband electron system is actually a set of 2D electron systems. Therefore, the single factor  $S(q, \omega)$  is not appropriate for description of inter-subband electron scattering. Luckily, for non-interacting electrons, we can easily find an extension of  $S(q, \omega)$  which could be used in expressions for average scattering probabilities of a multisubband system:

$$S_{l,l'}(q, \omega) = \frac{2}{\pi \hbar Z_{\parallel}} \sum_{n,n'} \int d\varepsilon e^{-\varepsilon/T_e} J_{n,n'}^2(x_q) \times \text{Im} G_{l,n}(\varepsilon) \text{Im} G_{l',n'}(\varepsilon + \hbar\omega), \quad (7)$$

where

$$J_{n,n'}^2(x) = \frac{[\min(n, n')!]}{[\max(n, n')!]} x^{|n-n'|} e^{-x} \left[ L_{\min(n, n')}^{|n-n'|}(x) \right]^2,$$

$x_q = q^2 l_B^2 / 2$ , and  $L_n^m(x)$  are the associated Laguerre polynomials. The factor  $S_{l,l'}(q, \omega)$  contains the level densities at the initial and the final states, and it includes averaging over initial in-plane states. At  $l = l'$ , this factor coincides with the DSF of a nondegenerate 2D system of non-interacting electrons. Generally,  $S_{l,l'}(q, \omega)$  is not the dynamical structure factor of the whole system, nevertheless this function is very useful for description of dissipative processes in presence of MW irradiation.

As a useful example, consider the average inter-subband scattering rate  $\bar{\nu}_{l \rightarrow l'}$  caused by quasi-elastic scattering, which is important for obtaining subband occupancies  $\bar{n}_l = N_l / N_e$  under the MW resonance<sup>17</sup>. Using the damping theoretical formulation<sup>14</sup> and the SCBA<sup>13</sup>,  $\bar{\nu}_{l \rightarrow l'}$  can be represented in the following form

$$\bar{\nu}_{l \rightarrow l'} = \frac{\hbar}{m_e A} \sum_q \chi_{l,l'}(q) S_{l,l'}(q, \omega_{l,l'}), \quad (8)$$

where  $\chi_{l,l'} (= \chi_{l',l})$  describes electron coupling with scatterers. For SEs on liquid helium, we have two kinds of scatterers: ripples and vapor atoms. Therefore,  $\chi_{l,l'} = \chi_{l,l'}^{(r)} + \chi_{l,l'}^{(a)}$ . Electron-ripple scattering gives

$$\chi_{l,l'}^{(r)}(q) = \frac{m_e}{\hbar^3} Q_q^2 2N_q \left| (U_q)_{l,l'} \right|^2 \simeq \frac{m_e T}{\alpha \hbar^3 q^2} \left| (U_q)_{l,l'} \right|^2, \quad (9)$$

where  $N_q = (e^{\hbar\omega_q/T} - 1)^{-1} \gg 1$ , and  $(U_q)_{l,l'} \equiv \langle l | U_q(z_e) | l' \rangle$ . For electron scattering at vapor atoms,

$$\chi_{l,l'}^{(a)}(q) = \nu_0^{(a)} p_{l,l'}, \quad \nu_0^{(a)} = \frac{m_e n_a^{(3D)} (V^{(a)})^2}{\hbar^3 B_{1,1}} \quad (10)$$

where

$$p_{l,l'} = \frac{B_{1,1}}{B_{l,l'}}, \quad B_{l,l'}^{-1} = L_z^{-1} \sum_{K_z} \left| (e^{iK_z z_e})_{l,l'} \right|^2,$$

$L_z$  is the height above the liquid surface,  $n_a^{(3D)}$  is the density of vapor atoms, and  $K_z$  is the projection of the vapor

atom wave-vector. The  $\nu_0^{(a)}$  represents the SE collision frequency at vapor atoms for  $B = 0$ .

The generalized factor of a multi-subband 2D electron system  $S_{l,l'}(q, \omega)$  will be used throughout this work because its basic property

$$S_{l,l'}(q, -\omega) = e^{-\hbar\omega/T_e} S_{l',l}(q, \omega) \quad (11)$$

allows us straightforwardly to obtain terms responsible for negative dissipation. This property follows from the detailed balancing for quasi-elastic processes,  $\bar{\nu}_{l' \rightarrow l} = e^{-\Delta_{l,l'}/T_e} \bar{\nu}_{l \rightarrow l'}$ , and also directly from the definition of Eq. (7). Using Gaussian level shapes of Eq. (6), one can find

$$S_{l,l'}(q, \omega) = \frac{2\pi^{1/2} \hbar}{Z_{\parallel}} \sum_{n,n'} \frac{J_{n,n'}^2(x_q)}{\Gamma_{l,n;l',n'}} e^{-\varepsilon_n/T_e} I_{l,n;l',n'}(\omega), \quad (12)$$

where  $2\Gamma_{l,n;l',n'}^2 = \Gamma_{l,n}^2 + \Gamma_{l',n'}^2$ , and

$$I_{l,n;l',n+m}(\omega) = \exp \left[ - \left( \frac{\hbar\omega - m\hbar\omega_c - \Gamma_{l,n}^2/4T_e}{\Gamma_{l,n;l',n+m}} \right)^2 + \frac{\Gamma_{l,n}^2}{8T_e^2} \right]. \quad (13)$$

The  $S_{l,l'}(q, \omega)$ , as a function of frequency, has sharp maxima when  $\omega$  equals the in-plane excitation energy  $(n' - n)\hbar\omega_c$ . The parameter  $\Gamma_{l,n;l',n'}^2$  describes broadening of these maxima. Eqs. (12) and (13) satisfy the condition of Eq. (11). Terms of the order of  $(\Gamma_{l,n}/T_e)^2$  entering the argument of Eq. (13) could be omitted, as it was done for  $Z_{\parallel}$ , because even the linear in  $\Gamma_{l,n}/T_e$  term provides us the necessary condition of Eq. (11). Anyway, our final results will be represented in forms which allow to disregard even the linear in  $\Gamma_{l,n}/T_e$  term entering  $I_{l,n;l',n'}(\omega)$ .

Consider the decay rate of the first excited subband  $\bar{\nu}_{2 \rightarrow 1}$ . Under typical experimental condition,  $\Gamma_{l,n;l',n'}$  is much smaller than  $\hbar\omega_c$ . Therefore, most of terms entering  $S_{l,l'}(q, \omega_{2,1})$  are exponentially small and can be disregarded. The exceptional terms satisfy the condition  $n' - n = m^*(B)$ , where  $m^*(B) \equiv \text{round}(\omega_{2,1}/\omega_c)$  is an integer nearest to  $\omega_{2,1}/\omega_c$ . In this notation,

$$\bar{\nu}_{2 \rightarrow 1} = \sum_{n=0}^{\infty} \frac{e^{-\varepsilon_n/T_e}}{Z_{\parallel}} \frac{\hbar\omega_c \beta_{2,n;1,n+m^*}}{\pi^{1/2} \Gamma_{2,n;1,n+m^*}^2} \times \exp \left\{ - \frac{\hbar^2 (\omega_{2,1} - m^* \omega_c)^2}{\Gamma_{2,n;1,n+m^*}^2} \right\}, \quad (14)$$

where

$$\beta_{l,n;l',n+m} = \int_0^{\infty} \chi_{l,l'} J_{n,n+m}^2(x_q) dx_q.$$

For electron scattering at vapor atoms,  $\beta_{l,n;l',n+m} \equiv \beta_{l,l'}^{(a)} = \nu_0^{(a)} p_{l,l'}$  which coincides with  $\chi_{l,l'}^{(a)}$ . In the case of electron-ripple scattering,  $\beta_{2,n;1,n+m}$  has a more complicated expression due to a particular form of  $U_q(z_e)$

entering the definition of  $\chi_{l,l'}^{(r)}$ . The  $\bar{\nu}_{2 \rightarrow 1}(B)$  is a  $1/B$ -periodic function. It has sharp maxima when  $\omega_{2,1}/\omega_c$  equals an integer. In the argument of the exponential function of Eq. (14), we have disregarded terms which are small for  $\Gamma_{l,n}/T_e \ll 1$ .

Transition rates  $\bar{\nu}_{l \rightarrow l'}$  determine subband occupancies  $\bar{n}_l$  under the MW resonance. At low electron temperatures, the two-subband model is applicable, and the rate equation gives

$$\frac{\bar{n}_2}{\bar{n}_1} = \frac{r + e^{-\Delta_{2,1}/T_e} \bar{\nu}_{2 \rightarrow 1}}{r + \bar{\nu}_{2 \rightarrow 1}}, \quad (15)$$

where  $r$  is the stimulated absorption (emission) rate due to the MW field, and  $\bar{n}_1 + \bar{n}_2 = 1$ . Thus, under the MW resonance, magnetooscillations of  $\bar{\nu}_{2 \rightarrow 1}$  lead to magnetooscillations of subband occupancies  $\bar{n}_1$  and  $\bar{n}_2$ . For further analysis, it is important that MW excitation provides the condition  $\bar{n}_2 > \bar{n}_1 e^{-\Delta_{2,1}/T_e}$ , which is the main cause of negative momentum dissipation.

### III. MAGNETOCONDUCTIVITY UNDER RESONANCE MW IRRADIATION

Consider now an infinite isotropic multisubband 2D electron system under an in-plane dc-electric field, assuming arbitrary occupancies of surface subbands  $\bar{n}_l$  induced by the MW resonance. In the linear transport regime, the average friction force acting on electrons due to interaction with scatterers  $\mathbf{F}_{\text{scat}}$  is proportional to the average electron velocity  $\mathbf{V}_{\text{av}} = \langle \mathbf{v}_e \rangle$ . This relationship can be conveniently written as  $\mathbf{F}_{\text{scat}} = -N_e m_e \nu_{\text{eff}} \mathbf{V}_{\text{av}}$ , where the proportionality factor  $\nu_{\text{eff}}$  represents an effective collision frequency which depends on  $B$  and, generally, on electron density. The  $\mathbf{F}_{\text{scat}}$  is balanced by the average Lorentz force  $\langle \mathbf{F}_{\text{field}} \rangle$ , which yields the usual Drude form for the electron conductivity tensor  $\sigma_{i,k}$ , where the quasi-classical collision frequency  $\nu_0$  is substituted for  $\nu_{\text{eff}}$ <sup>11,16</sup>.

The effective collision frequency  $\nu_{\text{eff}}$  can be obtained directly from the expression for the average momentum gained by scatterers per unit time. Usually, to describe momentum relaxation, one has to obtain deviations of

the in-plane electron distribution function from the simple form of Eq. (2) induced by the dc-electric field. For the highly correlated 2D system of SEs on liquid helium under magnetic field, this problem was solved in a general way, assuming that in the center-of-mass reference frame the electron DSF has its equilibrium form  $S^{(0)}(q, \omega)$ . In the laboratory frame, its frequency argument acquires the Doppler shift  $S(\mathbf{q}, \omega) = S^{(0)}(q, \omega - \mathbf{q} \cdot \mathbf{V}_{\text{av}})$  due to Galilean invariance<sup>11,16</sup>. This approach is similar to the description of electron transport by a velocity shifted Fermi-function of the kinetic equation method, where  $\mathbf{V}_{\text{av}}$  is found from the momentum balance equation. The same properties can be ascribed to the generalized factor<sup>10</sup>  $S_{l,l'}(\mathbf{q}, \omega)$ .

Here, we consider a different way, taking into account that  $\mathbf{F}_{\text{scat}}$ , as well as the momentum gained by scatterers, can be evaluated in any inertial reference frame. We choose the reference frame fixed to the electron liquid center-of-mass, because in it the in-plane distribution function of highly correlated electrons ( $\nu_{ee} \gg \nu_{\text{eff}}$ ) has its simplest form of Eq. (2), and the generalized factor  $S_{l,l'}(\mathbf{q}, \omega)$  has its equilibrium form of Eq. (7). Then,  $\mathbf{F}_{\text{scat}}$  can be considered as the drag due to moving scatterers. At the same time, distribution functions of scatterers which are not affected by external fields can be easily found according to well-known rules.

In the electron liquid center-of-mass reference frame, the in-plane spectrum of electrons is close to the Landau spectrum, because the driving electric field  $\mathbf{E}' = \mathbf{E} - (1/c)\mathbf{B} \times \mathbf{V}_{\text{av}}$  is nearly zero, at least for  $\omega_c \gg \nu_{\text{eff}}$ . At the same time, in this frame the ripplon excitation energy is changed to  $E_{\mathbf{q}}^{(r)} = \hbar\omega_{\mathbf{q}} - \hbar\mathbf{q}\mathbf{V}_{\text{av}}$ , because the gas of ripples moves as a whole with the drift velocity equal to  $-\mathbf{V}_{\text{av}}$ . The same Doppler shift correction  $-\hbar\mathbf{q}\mathbf{V}_{\text{av}}$  appears for the energy exchange in the case of electron scattering at vapor atoms, even for the limiting case  $M \rightarrow \infty$  (impurities which are motionless in the laboratory reference frame). In the electron center-of-mass reference frame, vapor atoms move with the velocity  $-\mathbf{V}_{\text{av}}$  and hit electrons which results in the energy exchange  $-\hbar\mathbf{q}\mathbf{V}_{\text{av}}$ .

Describing electron-riplon scattering probabilities in terms of the equilibrium factor  $S_{l,l'}(q, \omega)$ , as discussed above, contributions to the frictional force from creation and destruction processes can be found as

$$\mathbf{F}_{\text{scat}} = -\frac{N_e}{\hbar^2 A} \sum_{\mathbf{q}} \hbar\mathbf{q} Q_q^2 \sum_{l,l'} \bar{n}_l \left| (U_q)_{l,l'} \right|^2 \left[ (N_{\mathbf{q}} + 1) S_{l,l'}(q, \omega_{l,l'} - E_{\mathbf{q}}^{(r)}/\hbar) - N_{\mathbf{q}} S_{l,l'}(q, \omega_{l,l'} + E_{\mathbf{q}}^{(r)}/\hbar) \right]. \quad (16)$$

It is clear that disregarding the Doppler-shift correction  $-\hbar\mathbf{q}\mathbf{V}_{\text{av}}$  in this equation yields zero result. This correction enters the ripplon distribution function  $N_{\mathbf{q}}$  and the frequency argument of the factor  $S_{l,l'}$ . In the linear transport regime, the Doppler-shift correction entering

the ripplon distribution function is unimportant. This can be seen directly from Eq. (16): setting  $E_{\mathbf{q}}^{(r)} \rightarrow 0$  in the frequency argument of  $S_{l,l'}$  gives zero result for  $\mathbf{F}_{\text{scat}}$ . Therefore, in this equation one can substitute  $N_{\mathbf{q}}$  for  $N_q$  defined in Eq. (9). We can also disregard  $\hbar\omega_q$  in

the frequency argument of  $S_{l,l'}$ . Then, interchanging the running indices of the second term in the square brackets, and using the basic property of  $S_{l,l'}(q, \omega)$  given in Eq. (11), Eq. (16) can be represented as

$$\mathbf{F}_{\text{scat}} = -\frac{N_e \hbar}{2m_e A} \sum_{l,l'} \sum_{\mathbf{q}} \hbar \mathbf{q} \chi_{l,l'}(q) S_{l,l'}(q, \omega_{l,l'} + \mathbf{q} \cdot \mathbf{V}_{\text{av}}) \times \left( \bar{n}_l - \bar{n}_{l'} e^{-\Delta_{l,l'}/T_e} e^{-\hbar \mathbf{q} \cdot \mathbf{V}_{\text{av}}/T_e} \right), \quad (17)$$

where  $\chi_{l,l'}(q) = \chi_{l,l'}^{(r)}(q)$  was defined in Eq. (9). This equation has the most convenient form for expansion in  $\hbar \mathbf{q} \cdot \mathbf{V}_{\text{av}}$ .

A similar equation for  $\mathbf{F}_{\text{scat}}$  can be found considering electron scattering at vapor atoms. Evaluating momentum relaxation rate, one can disregard  $\hbar \chi_{\mathbf{K},\mathbf{K}'} = \varepsilon_{\mathbf{K}'-\mathbf{K}}^{(a)} - \varepsilon_{\mathbf{K}'}^{(a)}$  which represents the energy exchange at a collision in the laboratory reference frame. In the center-of-mass reference frame, Doppler-shift corrections enter the vapor atom distribution function  $N_{\mathbf{K}'}^{(a)}$  and the frequency argument of the factor  $S_{l,l'}$  due to the new energy exchange at a collision  $-\hbar \mathbf{q} \cdot \mathbf{V}_{\text{av}}$ . The correction entering  $N_{\mathbf{K}'}^{(a)}$  is unimportant because of the normalization condition:  $\sum_{\mathbf{K}'} N_{\mathbf{K}'}^{(a)} = n_a^{(3D)} L_z A$ . Therefore, we have

$$\mathbf{F}_{\text{scat}} = -\frac{N_e \hbar \nu_0^{(a)}}{m_e A} \sum_{l,l'} \bar{n}_l p_{l,l'} \times \sum_{\mathbf{q}} \hbar \mathbf{q} S_{l,l'}(q, \omega_{l,l'} + \mathbf{q} \cdot \mathbf{V}_{\text{av}}). \quad (18)$$

In order to obtain the form of Eq. (17), we represent the right side of Eq. (18) as a sum of two identical halves and change the running indices in the second half:  $\mathbf{q} \rightarrow -\mathbf{q}$  and  $l \rightleftharpoons l'$ . Then, the basic property of  $S_{l,l'}(q, \omega)$  yields Eq. (17) with  $\chi_{l,l'} = \chi_{l,l'}^{(a)}$ , where  $\chi_{l,l'}^{(a)}$  is from Eq. (10).

Thus, Eq. (17) is applicable for both scattering mechanisms. In the general case,  $\chi_{l,l'} = \chi_{l,l'}^{(r)} + \chi_{l,l'}^{(a)}$ . The effective collision frequency under magnetic field  $\nu_{\text{eff}}$  can be found expanding Eq. (17) in  $\mathbf{q} \cdot \mathbf{V}_{\text{av}}$  up to linear terms. We shall represent  $\nu_{\text{eff}}$  as a sum of two different contributions:  $\nu_{\text{eff}} = \nu_{\text{N}} + \nu_{\text{A}}$ . The normal contribution  $\nu_{\text{N}}$  originates from the expansion of the exponential factor  $\exp(-\hbar \mathbf{q} \cdot \mathbf{V}_{\text{av}}/T_e)$ . In turn,  $\nu_{\text{N}}$  can be represented as a sum of contributions from intra-subband and inter-subband scattering  $\nu_{\text{N}} = \nu_{\text{N},\text{intra}} + \nu_{\text{N},\text{inter}}$ . The sums of  $\nu_{\text{N},\text{inter}}$  take account of all  $l, l'$ . It is useful to rearrange terms with  $l < l'$  ( $\Delta_{l,l'} < 0$ ) by interchanging the running indices  $l \rightleftharpoons l'$ , and using the basic property of

$S_{l,l'}(q, \omega)$ . Then, we have

$$\nu_{\text{N},\text{intra}} = \frac{\hbar \omega_c^2}{4\pi T_e} \sum_l \bar{n}_l \int_0^\infty x_q \chi_{l,l}(q) S_{l,l}(q, 0) dx_q, \quad (19)$$

$$\nu_{\text{N},\text{inter}} = \frac{\hbar \omega_c^2}{4\pi T_e} \sum_{l>l'} \left( \bar{n}_l + \bar{n}_{l'} e^{-\Delta_{l,l'}/T_e} \right) \times \int_0^\infty x_q \chi_{l,l'}(q) S_{l,l'}(q, \omega_{l,l'}) dx_q. \quad (20)$$

The  $\nu_{\text{N}}(B)$  is always positive. In the limiting case of a one-subband 2D electron system ( $\bar{n}_l = \delta_{l,1}$ ), Eq. (19) reproduces the known relationship between the effective collision frequency and the electron DSF<sup>11</sup>. In the parentheses of Eq. (20), the first term is due to scattering from  $l$  to  $l'$ , while the second term describes the contribution of scattering back from  $l'$  to  $l$ . It should be noted that the forms of Eqs. (19) and (20) allow to simplify  $S_{l,l'}(q, \omega_{l,l'})$  of Eq. (12) by disregarding small corrections proportional to  $\Gamma_{l,n}/T_e$  and  $(\Gamma_{l,n}/T_e)^2$  entering  $I_{l,n;l',n'}(\omega)$  defined by Eq. (13).

The anomalous contribution to the effective collision frequency  $\nu_{\text{A}}(B)$  can be found from Eq. (17) expanding  $S_{l,l'}(q, \omega_{l,l'} + \mathbf{q} \cdot \mathbf{V}_{\text{av}})$  in  $\mathbf{q} \cdot \mathbf{V}_{\text{av}}$ , and setting  $\exp(-\hbar \mathbf{q} \cdot \mathbf{V}_{\text{av}}/T_e) \rightarrow 1$  in the parentheses. In this case, to rearrange terms with  $l < l'$  ( $\Delta_{l,l'} < 0$ ), we shall use the property

$$S'_{l',l}(q, -\omega) = -e^{-\frac{\hbar \omega}{T_e}} S'_{l,l'}(q, \omega) + \frac{\hbar}{T_e} e^{-\frac{\hbar \omega}{T_e}} S_{l,l'}(q, \omega) \simeq -e^{-\frac{\hbar \omega}{T_e}} S'_{l,l'}(q, \omega). \quad (21)$$

Here  $S'_{l,l'}(q, \omega) \equiv \partial S_{l,l'}(q, \omega) / \partial \omega$ , and the last transformation assumes that  $\Gamma_{l,n} \ll T_e$ . Interchanging the running indices  $l \rightleftharpoons l'$  of terms with  $\Delta_{l,l'} < 0$  and using Eq. (21),  $\nu_{\text{A}}(B)$  can be found as

$$\nu_{\text{A}} = \frac{\omega_c^2}{2\pi} \sum_{l>l'} \left( \bar{n}_l - \bar{n}_{l'} e^{-\Delta_{l,l'}/T_e} \right) \times \int_0^\infty x_q \chi_{l,l'}(q) S'_{l,l'}(q, \omega_{l,l'}) dx_q. \quad (22)$$

As compared to  $\nu_{\text{N},\text{inter}}$  of the normal contribution, here the second term in parentheses has the opposite sign. Therefore, for usual Boltzmann distribution of subband occupancies,  $\nu_{\text{A}}(B) = 0$ . The anomalous contribution appears only when  $\bar{n}_l \neq \bar{n}_{l'} e^{-\Delta_{l,l'}/T_e}$ , which occurs under the MW resonance condition  $\omega = \omega_{l,l'}$ .

In the form of Eq. (22), it is possible to use a simplified expression

$$S'_{l,l'}(q, \omega_{l,l'}) \simeq -\frac{2\pi^{1/2} \hbar}{Z_{\parallel}} \sum_{n,n'} \frac{J_{n,n'}^2(x_q)}{\Gamma_{l,n;l',n'}} e^{-\varepsilon_n/T_e} \exp \left\{ -\frac{[\Delta_{l,l'} - (n' - n) \hbar \omega_c]^2}{\Gamma_{l,n;l',n'}^2} \right\} \frac{2\hbar^2 [\omega_{l,l'} - (n' - n) \omega_c]}{\Gamma_{l,n;l',n'}^2}, \quad (23)$$

which disregards terms proportional to  $\Gamma_{l,n}/T_e$  and  $(\Gamma_{l,n}/T_e)^2$ . From Eqs. (22) and (23) one can see that at  $\bar{n}_l > \bar{n}_{l'} e^{-\Delta_{l,l'}/T_e}$ , the sign of  $\nu_A(B)$  is opposite to the sign of  $\omega_{l,l'} - (n' - n)\omega_c$ . Therefore,  $\nu_A(B) < 0$  when the magnetic field  $B$  is slightly lower the commensurability condition  $\Delta_{2,1}/\hbar\omega_c = m$  (here  $m$  is an integer), which agrees with the experimental observation for minima of  $\sigma_{xx}$ .

For further analysis, it is convenient to introduce

$$\lambda_{l,n;l',n'} = \int_0^\infty x_q \chi_{l,l'}(q) J_{n,n'}^2(x_q) dx_q. \quad (24)$$

When referring to a particular scattering mechanism, we shall use a superscript,  $\lambda_{l,n;l',n'} = \lambda_{l,n;l',n'}^{(r)} + \lambda_{l,n;l',n'}^{(a)}$ . Consider a two-subband model which is valid at low enough electron temperatures. Using the new definitions given above, the normal contribution to the effective collision frequency can be represented as

$$\nu_{N,intra} = \sum_{n=0}^{\infty} \frac{e^{-\varepsilon_n/T_e} (\hbar\omega_c)^2}{2\sqrt{\pi}T_e Z_{\parallel}} \left[ \bar{n}_1 \frac{\lambda_{1,n;1,n}}{\Gamma_{1,n}} + \bar{n}_2 \frac{\lambda_{2,n;2,n}}{\Gamma_{2,n}} \right], \quad (25)$$

$$\begin{aligned} \nu_{N,inter} &= \left( \bar{n}_2 + \bar{n}_1 e^{-\Delta_{2,1}/T_e} \right) \frac{(\hbar\omega_c)^2}{2\sqrt{\pi}T_e} \sum_{n=0}^{\infty} \frac{e^{-\varepsilon_n/T_e}}{Z_{\parallel}} \times \\ &\times \frac{\lambda_{2,n;1,n+m^*}}{\Gamma_{2,n;1,n+m^*}} \exp \left[ -\frac{\hbar^2 (\omega_{2,1} - m^* \omega_c)^2}{\Gamma_{2,n;1,n+m^*}^2} \right], \end{aligned} \quad (26)$$

where  $m^* \equiv \text{round}(\omega_{2,1}/\omega_c)$  is the function of  $B$  defined in the previous Section. The  $\nu_{N,intra}$  and  $\nu_{N,inter}$  have magnetooscillations of two kinds. Oscillations of  $\nu_{N,inter}$  are quite obvious, because quasi-elastic inter-subband scattering increases sharply at the commensurability condition:  $\omega_{2,1} = m\omega_c$ . The shape of these peaks is symmetrical with respect to the point  $\Delta_{2,1}/\hbar\omega_c = m$ . It is formed by the interplay of the exponential factor, having  $\Gamma_{2,n;1,n+m^*}$  for the broadening parameter, and the line-shapes of the subband occupancies. It should be noted that at low electron temperatures,  $\nu_{N,inter}$  is exponentially small. The intra-subband scattering contribution  $\nu_{N,intra}$  oscillates with  $1/B$  in an indirect way because of oscillations in level occupancies  $\bar{n}_2$  and  $\bar{n}_1$  induced by oscillations in the decay rate  $\bar{\nu}_{2 \rightarrow 1}$ , according to Eqs. (14) and (15). These oscillations have also a symmetrical shape whose broadening is affected by the relation between  $r$  and  $\bar{\nu}_{2 \rightarrow 1}$ .

Magnetooscillations of  $\nu_A(B)$  have a completely different shape:

$$\begin{aligned} \nu_A &= - \left( \bar{n}_2 - \bar{n}_1 e^{-\Delta_{2,1}/T_e} \right) \frac{(\hbar\omega_c)^2}{\sqrt{\pi}} \times \\ &\times \sum_{n=0}^{\infty} \frac{e^{-\varepsilon_n/T_e}}{Z_{\parallel}} \frac{\lambda_{2,n;1,n+m^*}}{\Gamma_{2,n;1,n+m^*}^2} \times \\ &\times \exp \left[ -\frac{\hbar^2 (\omega_{2,1} - m^* \omega_c)^2}{\Gamma_{2,n;1,n+m^*}^2} \right] \frac{2\hbar (\omega_{2,1} - m^* \omega_c)}{\Gamma_{2,n;1,n+m^*}}, \end{aligned} \quad (27)$$

In the ultra-quantum limit  $\hbar\omega_c \gg T_e$ , terms with  $n > 0$  entering Eq. (27) can be omitted, which allows to describe magneto-oscillations of  $\nu_A(B)$  in an analytical form. In contrast with oscillations of the normal contribution  $\nu_N$ , in the vicinity of the commensurability condition,  $\nu_A$  is an odd function of  $\omega_{2,1}/\omega_c - m^*$ .

Thus, the effective collision frequency  $\nu_{\text{eff}} = \nu_N + \nu_A$  and magnetoconductivity  $\sigma_{xx}$  of SEs are found for any given electron temperature. In order to obtain  $T_e$  as a function of the magnetic field, it is necessary to describe energy relaxation of SEs for arbitrary subband occupancies.

#### IV. ENERGY DISSIPATION

It is instructive to analyze another important example of negative dissipation which can be induced by the MW resonance. Consider the energy loss rate of a multisubband 2D electron system due to interaction with scatterers. In this case, there are no complications with the dc-driving electric field or with the Doppler shifts which can be set to zero. This analysis will be important also for description of electron heating due to decay of the SE state excited by the MW.

The energy loss rate per an electron due to one-rippelon creation and destruction processes can be represented in terms of  $S_{l,l'}(q, \omega)$  quite straightforwardly:

$$\begin{aligned} \dot{W} &= -\frac{1}{\hbar^2 A} \sum_{\mathbf{q}} \hbar\omega_{\mathbf{q}} Q_{\mathbf{q}}^2 (N_{\mathbf{q}} + 1) \sum_{l,l'} \left| (U_{\mathbf{q}})_{l,l'} \right|^2 \times \\ &\times \left[ \bar{n}_l S_{l,l'}(q, \omega_{l,l'} - \omega_{\mathbf{q}}) - \bar{n}_{l'} e^{-\hbar\omega_{\mathbf{q}}/T} S_{l,l'}(q, \omega_{l,l'} + \omega_{\mathbf{q}}) \right]. \end{aligned} \quad (28)$$

Interchanging the running indices ( $l, l'$ ) in the second term, and using the basic property of  $S_{l,l'}(q, \omega)$  given in Eq. (11), the terms entering the square brackets can be rearranged as

$$S_{l,l'}(q, \omega_{l,l'} - \omega_{\mathbf{q}}) \left[ \bar{n}_l - \bar{n}_{l'} e^{-\Delta_{l,l'}/T_e} e^{-\hbar\omega_{\mathbf{q}}(1/T - 1/T_e)} \right]. \quad (29)$$

Since the processes considered here are quasi-elastic, we can expand this equation in  $\hbar\omega_{\mathbf{q}}$  and represent  $\dot{W}$  as a sum of two different contributions:  $\dot{W} = \dot{W}_N + \dot{W}_A$ . The normal energy loss rate  $\dot{W}_N$  is proportional to  $T_e - T$ , which is a measure of deviation from the equilibrium,

$$\dot{W}_N = -\frac{(T_e - T)\hbar}{m_e A} \sum_{\mathbf{q}} \sum_{l,l'} \bar{n}_{l'} e^{-\Delta_{l,l'}/T_e} \tilde{\chi}_{l,l'}^{(r)} S_{l,l'}(q, \omega_{l,l'}), \quad (30)$$

Here

$$\tilde{\chi}_{l,l'}^{(r)} = \frac{m_e q}{2\rho\hbar T_e} \left| (U_{\mathbf{q}})_{l,l'} \right|^2.$$

This contribution originates from expansion of the exponential function in  $\hbar\omega_{\mathbf{q}}(1/T - 1/T_e)$ .

It is conventional to represent the energy loss as  $\dot{W}_N = -(T_e - T)\tilde{\nu}_N^{(r)}$ , where  $\tilde{\nu}_N^{(r)}$  is the energy relaxation rate of an electron. Rearranging terms with  $l < l'$  ( $\Delta_{l,l'} < 0$ ), as described in the previous Section, one can find

$$\begin{aligned} \tilde{\nu}_N^{(r)} &= \frac{\hbar}{m_e A} \sum_{\mathbf{q}} \sum_l \bar{n}_l \tilde{\chi}_{l,l}^{(r)} S_{l,l}(q, 0) + \\ &+ \frac{\hbar}{m_e A} \sum_{\mathbf{q}} \sum_{l>l'} \left( \bar{n}_l + \bar{n}_{l'} e^{-\Delta_{l,l'}/T_e} \right) \tilde{\chi}_{l,l'}^{(r)} S_{l,l'}(q, \omega_{l,l'}). \end{aligned} \quad (31)$$

The normal contribution  $\tilde{\nu}_N^{(r)}$  is always positive, which means positive dissipation ( $\dot{W}_N < 0$ ) regardless of subband occupancies  $\bar{n}_l$ .

An anomalous contribution  $\dot{W}_A$  appears when expanding  $S_{l,l'}(q, \omega_{l,l'} - \omega_q)$  of Eq. (29) in  $\omega_q$  and setting  $e^{-\hbar\omega_q(1/T-1/T_e)}$  to unity. The rearrangement of terms with  $l < l'$  ( $\Delta_{l,l'} < 0$ ) based on the property of Eq. (21) yields

$$\begin{aligned} \dot{W}_A &= \frac{2TT_e}{m_e A} \sum_{l>l'} \left( \bar{n}_l - \bar{n}_{l'} e^{-\Delta_{l,l'}/T_e} \right) \times \\ &\times \sum_{\mathbf{q}} \tilde{\chi}_{l,l'}^{(r)} S'_{l,l'}(q, \omega_{l,l'}). \end{aligned} \quad (32)$$

Here  $\bar{n}_l - \bar{n}_{l'} e^{-\Delta_{l,l'}/T_e}$  represents an additional measure of deviation from the equilibrium induced by the MW. For equilibrium distribution of fractional occupancies  $\bar{n}_l$ , the anomalous term equals zero, but for occupancies  $\bar{n}_2 > \bar{n}_1 e^{-\Delta_{2,1}/T_e}$  induced by the MW resonance,  $\dot{W}_A$  can lead to negative energy dissipation of the electron system. In Eq. (32), one can use the approximate expression for  $S'_{l,l'}(q, \omega_{l,l'})$  given in Eq. (23). According to Eqs. (23) and (32), the sign of  $-\dot{W}_A$  coincides with the sign of  $\omega_{2,1} - (n' - n)\omega_c$  which can be negative or positive depending on the magnetic field. Since  $\Gamma_{l,n;l',n'} \ll \hbar\omega_c < \Delta_{2,1}$ , the contribution  $\dot{W}_A$  is mostly exponentially small with the exception of magnetic fields where  $\Delta_{l,l'} - (n' - n)\hbar\omega_c \lesssim \Gamma_{l,n;l',n'}$ .

The appearance of negative corrections to energy dissipation under the condition  $\bar{n}_2 - \bar{n}_1 e^{-\Delta_{2,1}/T_e} > 0$  can be explained quite easily. The negative anomalous contribution ( $\dot{W}_A > 0$ ) corresponds to  $(n' - n)\hbar\omega_c > \Delta_{2,1}$ . For narrow Landau levels, this means that scattering from the excited subband ( $l = 2$ ) to the ground subband ( $l' = 1$ ) is accompanied by destruction of a ripplon, while the corresponding scattering back from the ground subband to the excited subband is accompanied by creation of a ripplon. When  $\bar{n}_2 = \bar{n}_1 e^{-\Delta_{2,1}/T_e}$ , these two processes compensate each other in the expression for  $\dot{W}_A$ . If  $\bar{n}_2 > \bar{n}_1 e^{-\Delta_{2,1}/T_e}$ , destruction of riplons dominates, which leads to negative dissipation. In the opposite case, when  $(n' - n)\hbar\omega_c < \Delta_{2,1}$ , creation of riplons dominates, which results in additional positive dissipation. It should be noted that the negative contribution to energy dissipation and negative momentum dissipation

occur at the opposite sides of the point  $\hbar\omega_c = \Delta_{2,1}/m$ . Comparing Eq. (17) with Eqs. (28) and (29) one can conclude that the origin of this difference is the negative sign of the Doppler-shift correction in the ripplon excitation spectrum considered in the center-of-mass reference frame:  $E_{\mathbf{q}}^{(r)} = \hbar\omega_{\mathbf{q}} - \hbar\mathbf{q}\mathbf{V}_{\text{av}}$ .

Consider now the energy loss rate of SEs due to electron scattering at vapor atoms. In this case, the interaction Hamiltonian is proportional to the density fluctuation operator of vapor atoms  $\rho_{\mathbf{K}} = \sum_{\mathbf{K}'} a_{\mathbf{K}'-\mathbf{K}}^\dagger a_{\mathbf{K}'}$ , where  $\mathbf{K} = \{K_z, \mathbf{q}\}$  represents the momentum exchange between an electron and a scatterer. In terms of  $S_{l,l'}^{(0)}(q, \omega)$ , the energy loss rate per an electron can be obtained as

$$\begin{aligned} \dot{W} &= -\frac{(V^{(a)})^2}{A^2 L_z^2 \hbar} \sum_{l,l'} \bar{n}_l \sum_{\mathbf{K}', \mathbf{K}} \varkappa_{\mathbf{K}, \mathbf{K}'} \left| (e^{iK_z z_e})_{l,l'} \right|^2 \times \\ &\times N_{\mathbf{K}'}^{(a)} S_{l,l'}(q, \omega_{l,l'} - \varkappa_{\mathbf{K}, \mathbf{K}'}), \end{aligned} \quad (33)$$

where  $\hbar\varkappa_{\mathbf{K}, \mathbf{K}'} = \varepsilon_{\mathbf{K}'-\mathbf{K}}^{(a)} - \varepsilon_{\mathbf{K}'}^{(a)}$  is the energy exchange at a collision. In order to obtain  $\dot{W}_N$  and  $\dot{W}_A$ , we shall firstly rewrite Eq. (33) trivially as a sum of two identical halves. Then, in the second half, the running indices  $\mathbf{K}', \mathbf{K}$  will be substituted as  $\mathbf{K}' - \mathbf{K} \rightarrow \tilde{\mathbf{K}}'$ , and  $\mathbf{K} \rightarrow -\tilde{\mathbf{K}}$ , which changes the sign of the energy exchange,  $\varkappa_{\mathbf{K}, \mathbf{K}'} \rightarrow -\varkappa_{\tilde{\mathbf{K}}, \tilde{\mathbf{K}}'}$ . The next steps are the same as those resulting in Eq. (29). Interchanging the running indices  $l \rightleftharpoons l'$  in the second half, and using the basic property of  $S_{l,l'}^{(0)}(q, \omega)$  one can find

$$\begin{aligned} \dot{W} &= -\frac{(V^{(a)})^2}{2A^2 L_z^2 \hbar} \sum_{l,l'} \sum_{\mathbf{K}', \mathbf{K}} \varkappa_{\mathbf{K}, \mathbf{K}'} \left| (e^{iK_z z_e})_{l,l'} \right|^2 N_{\mathbf{K}'}^{(a)} \\ &\times S_{l,l'}(q, \omega_{l,l'} - \varkappa_{\mathbf{K}, \mathbf{K}'}) \\ &\times \left[ \bar{n}_l - \bar{n}_{l'} e^{-\Delta_{l,l'}/T_e} e^{-\hbar\varkappa_{\mathbf{K}, \mathbf{K}'}(1/T-1/T_e)} \right]. \end{aligned} \quad (34)$$

This equation is more convenient for expansion in  $\varkappa_{\mathbf{K}, \mathbf{K}'}$  than Eq. (33).

Expanding Eq. (34) in  $\varkappa_{\mathbf{K}, \mathbf{K}'}$ , one can find again that  $\dot{W} = \dot{W}_N + \dot{W}_A$ , where  $\dot{W}_N$  and  $\dot{W}_A$  have the same forms as that given in Eqs. (30) and (32), where  $\tilde{\chi}_{l,l'}^{(r)}$  should be substituted for

$$\tilde{\chi}_{l,l'}^{(a)} = \frac{m_e (V^{(a)})^2}{2AL_z^2 TT_e \hbar} \sum_{\mathbf{K}', K_z} (\varkappa_{\mathbf{K}, \mathbf{K}'})^2 N_{\mathbf{K}'}^{(a)} \left| (e^{iK_z z_e})_{l,l'} \right|^2. \quad (35)$$

Using the condition  $K' \gg K$ , this equation can be simplified as

$$\tilde{\chi}_{l,l'}^{(a)} = \nu_0^{(a)} \frac{m_e}{M} \left( u_{l,l'} \frac{E_R}{T_e} + x_q \frac{\hbar\omega_c}{T_e} p_{l,l'} \right), \quad (36)$$

where

$$u_{l,l'} = \frac{a_B^2 B_{11}}{C_{l'l}}, \quad C_{l'l}^{-1} = \frac{1}{L_z} \sum_{K_z} K_z^2 \left| (e^{iK_z z_e})_{l,l'} \right|^2.$$

Expressions for  $C_{l'l}^{-1}$  and  $B_{l'l}^{-1}$  convenient for numerical evaluations were given in Refs. 12 and 18.

The energy loss  $\dot{W}$  transferred to vapor atoms and ripples is balanced by the energy taken from the MW field:  $\dot{W} = (\bar{n}_1 - \bar{n}_2) \Delta_{2,1} r$ , where  $r$  is the MW excitation rate defined by

$$r = \frac{1}{2} \frac{\Omega_R^2 \gamma}{(\omega - \omega_{2,1})^2 + \gamma^2}, \quad (37)$$

where  $\gamma$  is the half-width of the MW resonance, and  $\Omega_R$  is the Rabi frequency proportional to the amplitude of the MW field. It is clear that negative contribution of  $\dot{W}_A$  will be compensated by an increase in  $\dot{W}_N$  due to electron heating.

Some useful expressions for the SE energy relaxation rate obtained for arbitrary subband occupancies are given in the Appendix. It should be noted that negative contributions to energy dissipation discussed above appear only for quasi-elastic inter-subband scattering. For SEs above superfluid  $^4\text{He}$ , there are inelastic inter-subband scattering processes accompanying by simultaneous emission of two short wave-length ripples<sup>11,17</sup>. These processes cause strong additional energy relaxation. Experiments of Refs. 4 and 5, were performed for SEs on the free surface of Fermi-liquid  $^3\text{He}$ . For such a substrate, short wavelength capillary waves with  $q \gtrsim 10^7$  are so heavily damped that even the existence of ripples with such wave-numbers is doubtful.

## V. RESULTS AND DISCUSSIONS

### A. Vapor atom scattering regime

Electron scattering at vapor atoms represents the most simple case for the magnetotransport theory, because the collision broadening of Landau levels of the same subband ( $\Gamma_l$ ) is independent of the level number  $n$ . The same is obviously valid for the broadening of the generalized factor  $S_{l,l'}(q, \omega)$ , which now can be denoted as  $\Gamma_{l,l'}$ . Additionally, the parameter defined in Eq. (24) has a very simple form  $\lambda_{l,n;l',n+m}^{(a)} = \nu_0^{(a)} p_{l,l'} (2n + 1 + m)$  which greatly simplifies evaluations.

Consider electron temperature as a function of the magnetic field. It is defined by the energy balance equation which contains the MW excitation rate  $r$  given in Eq. (37). In turn,  $r$  depends on the half-width of the MW resonance  $\gamma$ , which was studied theoretically with no magnetic field and under a parallel magnetic field<sup>19</sup>. If  $\mathbf{B}$  is applied perpendicular to the surface,  $\gamma$  should also have  $1/B$ -oscillating terms, because inter-subband scattering increases when  $\Delta_{2,1}/\hbar\omega_c \rightarrow m$ . In our numerical evaluation, we shall use a qualitative extension of the result obtained for  $B = 0$ . According to this result,  $\gamma$  contains the contribution from intra-subband scattering  $\gamma_{22-11}$  and the contribution from inter-subband scattering  $\gamma_{2,1} = \bar{\nu}_{2 \rightarrow 1}/2$ . Under the magnetic field applied

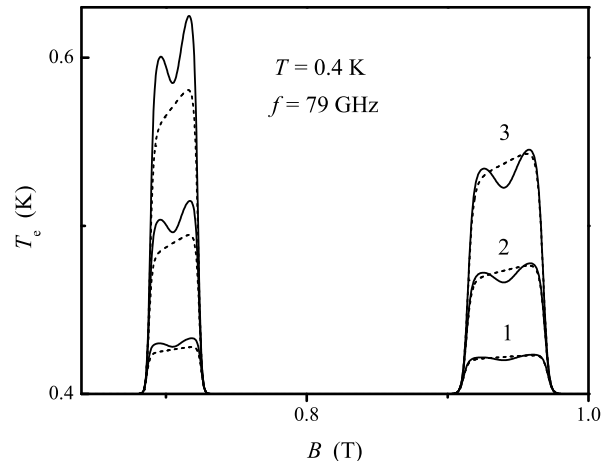


FIG. 1. Electron temperature vs the magnetic field for three levels of MW irradiation estimated at  $B = 1$  T:  $r = 10^5 \text{ s}^{-1}$  (1),  $3 \cdot 10^5 \text{ s}^{-1}$  (2), and  $5 \cdot 10^5 \text{ s}^{-1}$  (3). The solid curve was calculated for the model of  $\gamma(B)$  discussed in the text, the dashed curve represents the case  $r(B) = \text{const}$ .

normally, electron scattering is enhanced by the factor  $\hbar\omega_c/\sqrt{\pi}\Gamma_l$ <sup>13</sup>. Therefore, we can use an approximation

$$\gamma_{22-11} \approx \frac{\nu_0^{(a)} \hbar\omega_c}{2\sqrt{\pi}\Gamma_{2,1}} [p_{2,2} + p_{1,1} - 2p_{2,1}],$$

where  $\Gamma_{2,1}$  numerically is rather close to  $\Gamma_1 = \hbar\sqrt{2\omega_c\nu_0^{(a)}/\pi}$ . As for the oscillatory part  $\bar{\nu}_{2 \rightarrow 1}$  entering  $\gamma_{2,1}$ , we shall use the exact form of Eq. (14).

It should be noted that the oscillatory part of  $\gamma$  is not large because  $p_{2,1} \simeq 0.14$ . Still, it leads to some important consequences for electron temperature as a function of the magnetic field shown in Fig. 1. Solid curves represent results of numerical evaluations for the two-subband model taking into account oscillatory corrections to the MW resonance half-width  $\gamma$ , as described above. In this case, the electron temperature has small local minima at  $\Delta_{2,1}/\hbar\omega_c \rightarrow m$  due to oscillatory decrease in  $r \propto 1/\gamma$ . Three typical values of the Rabi frequency are chosen to provide MW excitation rate levels of  $10^5 \text{ s}^{-1}$ ,  $3 \cdot 10^5 \text{ s}^{-1}$  and  $5 \cdot 10^5 \text{ s}^{-1}$  at  $B = 1$  T. For a model with a constant MW excitation rate  $r$ , which is applicable when inhomogeneous broadening dominates, the corresponding results are shown by dashed curves. At  $\Delta_{2,1}/\hbar\omega_c \approx m$  these curves are nearly straight lines (without minima). For both models, the shape of curves describing the oscillatory increase of electron temperature has asymmetry with regard to the point  $\Delta_{2,1}/\hbar\omega_c = m$ . This asymmetry is due to the negative correction of the anomalous term  $\dot{W}_A$  leading to additional heating of the electron system at  $\hbar\omega_c > \Delta_{2,1}/m^*$ . The asymmetry increases strongly with the MW excitation rate  $r$  and with  $m^*(B)$ .

Electron heating increases with  $m^*$  (lowering  $B$ ), and,



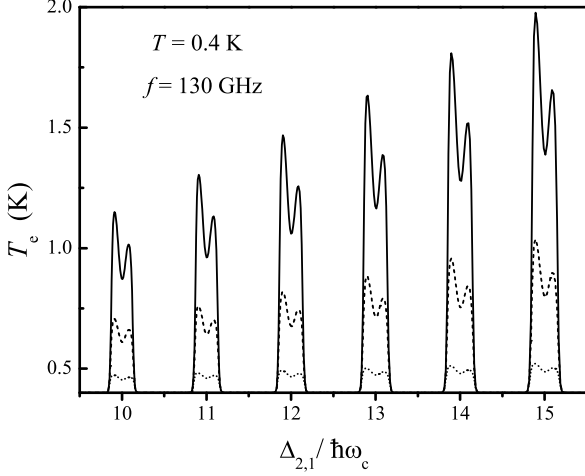


FIG. 2. Electron temperature vs  $\Delta_{2,1}/\hbar\omega_c$  for the MW of higher resonant frequency,  $f = 130$  GHz. Three levels of MW irradiation are the same as those described in the caption of Fig. 1. The all curves were calculated for the model of  $\gamma(B)$  discussed in the text.

for the excitation rate  $r = 5 \cdot 10^5 \text{ s}^{-1}$  at  $B = 1$  T, the two-subband model fails at  $m^* > 11$ . The applicability range of the two-subband model can be extended by using a stronger holding electric field which increases  $\Delta_{2,1}$ . In Fig. 2, electron temperature is shown as a function of the parameter  $\Delta_{2,1}/\hbar\omega_c \propto 1/B$  for a substantially higher MW frequency used in experiments on SEs<sup>20</sup>. For the solid curve, the two-subband model is applicable up to  $m^* = 15$ .

MW heating affects strongly the shape of conductivity oscillations because  $\nu_{\text{eff}}$  depends on electron temperature. For example, the normal contribution to the effective collision frequency can be represented as

$$\nu_{\text{N},\text{intra}}^{(a)} = \frac{\nu_0^{(a)} \hbar^2 \omega_c^2}{2\sqrt{\pi} T_e} \sum_l \frac{\bar{n}_l p_{l,l}}{\Gamma_{l,l}} \coth\left(\frac{\hbar\omega_c}{2T_e}\right), \quad (38)$$

$$\begin{aligned} \nu_{\text{N},\text{inter}}^{(a)} &= \frac{\nu_0^{(a)} \hbar^2 \omega_c^2}{2\sqrt{\pi} T_e} \sum_{l>l'} \left( \bar{n}_l^2 + \bar{n}_{l'} e^{-\Delta_{l,l'}/T_e} \right) \frac{p_{l,l'}}{\Gamma_{l,l'}} \times \\ &\times \left[ \coth\left(\frac{\hbar\omega_c}{2T_e}\right) F_{l,l'}(\omega_c) + H_{l,l'}(\omega_c) \right], \quad (39) \end{aligned}$$

where the new functions

$$F_{l,l'}(\omega_c) = \sum_{m=1}^{\infty} \exp\left[-\frac{\hbar^2(\omega_{l,l'} - m\omega_c)^2}{\Gamma_{l,l'}^2}\right], \quad (40)$$

$$H_{l,l'}(\omega_c) = \sum_{m=1}^{\infty} m \exp\left[-\frac{\hbar^2(\omega_{l,l'} - m\omega_c)^2}{\Gamma_{l,l'}^2}\right] \quad (41)$$

defined for  $l > l'$  are independent of  $T_e$ . For narrow Landau levels ( $\Gamma_{l,l'} \ll \hbar\omega_c$ ), the series defining  $F_{l,l'}$  or

$H_{l,l'}$  can be approximated by a single term with  $m = m^*$ , where  $m^*$  depends on the magnetic field according to the above noted rule:  $m^* = \text{round}(\omega_{l,l'}/\omega_c)$ .

The anomalous contribution to the effective collision frequency has a different form

$$\begin{aligned} \nu_{\text{A}}^{(a)} &= -\frac{\nu_0^{(a)} \hbar^2 \omega_c^2}{\pi^{1/2}} \sum_{l>l'} \left( \bar{n}_l - \bar{n}_{l'} e^{-\Delta_{l,l'}/T_e} \right) \frac{p_{l,l'}}{\Gamma_{l,l'}^2} \times \\ &\times \left[ \coth\left(\frac{\hbar\omega_c}{2T_e}\right) \Phi_{l,l'}(\omega_c) + \Theta_{l,l'}(\omega_c) \right], \quad (42) \end{aligned}$$

where functions  $\Phi_{l,l'}(\omega_c)$  and  $\Theta_{l,l'}(\omega_c)$  are defined similar to  $F_{l,l'}(\omega_c)$  and  $H_{l,l'}(\omega_c)$  of Eqs. (40) and (41) respectively, with the exception that their right sides contain the additional factor  $2\hbar(\omega_{l,l'} - m\omega_c)/\Gamma_{l,l'}$  originated from Eq. (23). Similar equations for SE energy relaxation rate are given in the Appendix.

Comparing  $T_e$ -dependencies of  $\nu_{\text{N}}^{(a)}$  and  $\nu_{\text{A}}^{(a)}$  given in Eqs. (38), (39) and (42), we conclude that heating of the electron system reduces the normal contribution to the effective collision frequency. In contrast with this, the anomalous sign-changing correction  $\nu_{\text{A}}^{(a)}$ , can be even enhanced to a some extent with heating of SEs due to the factor  $\coth(\hbar\omega_c/2T_e)$ . Typical magnetoconductivity oscillations of SEs calculated for the conditions of the experiment of Ref. 5 are shown in Fig. 3. Electron temperature calculated for these curves was shown in Fig. 1 by solid curves. At low MW excitation ( $r = 10^5 \text{ s}^{-1}$  at  $B = 1$  T), magnetooscillations of  $\sigma_{xx}$  are just simple maxima centered at  $\Delta_{2,1}/\hbar\omega_c = m$ , which agrees with experimental observations. Between the commensurability conditions,  $\sigma_{xx}$  is suppressed, as compared to the dash-dot-dot line calculated for zero MW power. This suppression is due to  $\bar{n}_2 \rightarrow \bar{n}_1 \rightarrow 1/2$  and weaker scattering at the excited subband. The increase in the decay rate  $\bar{\nu}_{2 \rightarrow 1}$  at  $\Delta_{2,1}/\hbar\omega_c \rightarrow m$  leads to a sharp decrease in  $\bar{n}_2$ , which restores  $\sigma_{xx}$  values obtained without the MW field. This restoration is not complete if  $T_e > T$ , because  $\nu_{\text{N},\text{intra}}^{(a)}$  decreases with heating, as discussed above. The  $\nu_{\text{N},\text{inter}}^{(a)}$  is very small under these conditions.

At higher MW excitation ( $r = 3 \cdot 10^5 \text{ s}^{-1}$  and  $5 \cdot 10^5 \text{ s}^{-1}$  at  $B = 1$  T), the shape of conductivity oscillations is affected strongly by the anomalous term  $\nu_{\text{A}}^{(a)}$  leading to local minima at  $\Delta_{2,1}/\hbar\omega_c > m$ . The  $\nu_{\text{A}}^{(a)}$  increases with  $r$  because of two reasons. The first reason is the increase in  $\Delta n = \bar{n}_2 - \bar{n}_1 e^{-\Delta_{2,1}/T_e}$  at higher MW excitation shown in Fig. 4. The second reason is electron heating due to decay of the excited SE state which increases  $\coth(\hbar\omega_c/2T_e)$  of Eq. (42). Further shape evolution is shown in Fig. 5 for larger  $m^*$  and  $f = 130$  GHz, where, according to Fig. 2, electron temperature can take a value of about 2 K. As expected, under these conditions the anomalous contribution strongly increases. Near the commensurability conditions  $\Delta_{2,1}/\hbar\omega_c \rightarrow m$ , the shape of conductivity oscillations becomes similar to that observed for the

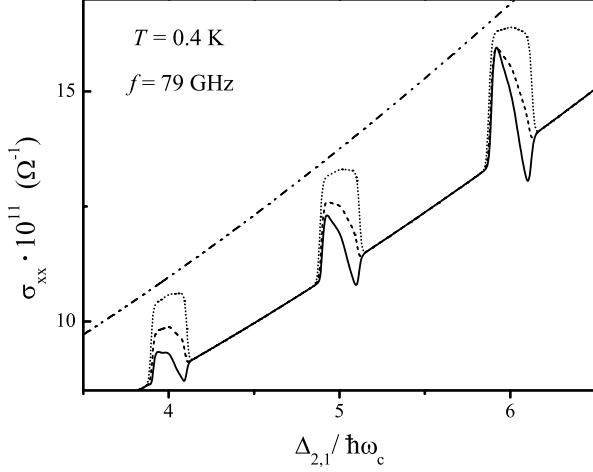


FIG. 3. Magnetoconductivity vs  $\Delta_{2,1}/\hbar\omega_c \propto 1/B$  for the MW of  $f = 79$  GHz. The dashed-dot-dot line was calculated with no MW irradiation. Dotted, dashed and solid curves represent three levels of MW irradiation ( $r$ ) given in the caption of Fig. 1.

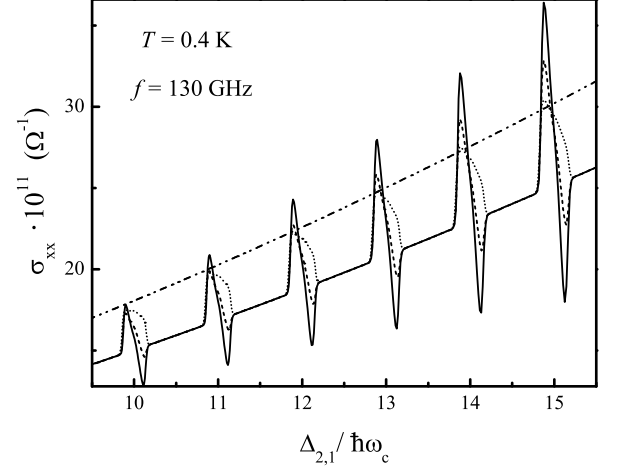


FIG. 5. Magnetoconductivity vs  $\Delta_{2,1}/\hbar\omega_c$  for the MW field of higher resonant frequency,  $f = 130$  GHz. The dashed-dot-dot line was calculated with no MW irradiation. Dotted, dashed and solid curves represent three levels of MW irradiation ( $r$ ) the same as those in Fig. 2.

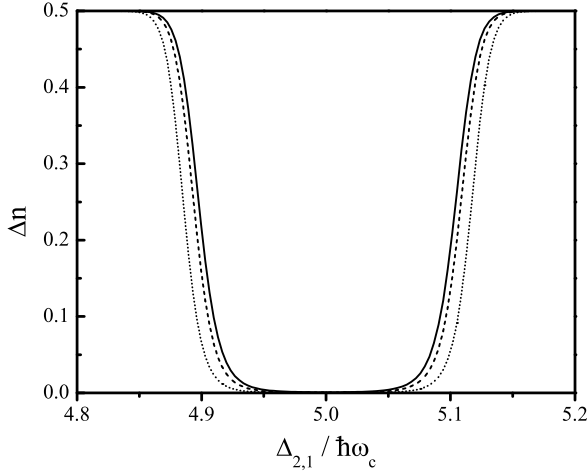


FIG. 4. Deviation of subband occupancies from the equilibrium distribution,  $\Delta n = \bar{n}_2 - \bar{n}_1 e^{-\Delta_{2,1}/T_e}$ , vs the parameter  $\Delta_{2,1}/\hbar\omega_c \propto 1/B$ . Dotted, dashed and solid curves represent three levels of MW irradiation ( $r$ ) given in the caption of Fig. 1.

electron-rippion scattering regime<sup>5</sup> at  $T = 0.2$  K. It is important that the results given in Fig. 5 are still obtained in the validity range of the two-subband model.

It is instructive to compare the peak broadening of different quantities shown in Fig. 6. The broadening of the decay rate  $\bar{\nu}_{2 \rightarrow 1}$  coincides with  $\Gamma_{2,1}$ , which is an average of  $\Gamma_2$  and  $\Gamma_1$ . In contrast, such quantities as  $|\nu_A|$ ,  $\bar{n}_1 - 1/2$ , and  $T_e - T$  rise in a much broader magnetic field range having nearly the same width which does

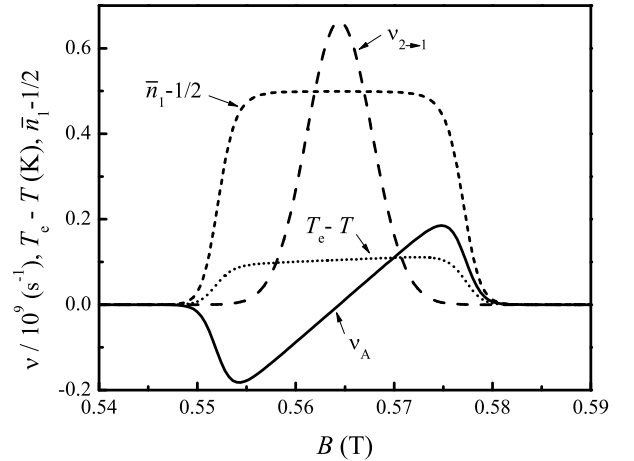


FIG. 6. Line shapes of  $\bar{\nu}_{2 \rightarrow 1}$  (dashed),  $\nu_A$  (solid),  $T_e - T$  (short-dotted), and  $\bar{n}_1 - 1/2$  (short-dashed) as functions of  $B$  near the commensurability point with  $m = 5$ , under the conditions:  $T = 0.4$  K, and  $r = 3 \cdot 10^5$  s<sup>-1</sup>.

not represent the broadening of Landau levels directly. We shall use this similarity in the line widths of  $T_e - T$  and  $\bar{n}_1 - 1/2$  later, considering electron heating for the electron-rippion scattering regime.

## B. Electron-rippion scattering regime

For electron-rippion scattering, the anomalous (sign-changing) contribution to the effective collision frequency

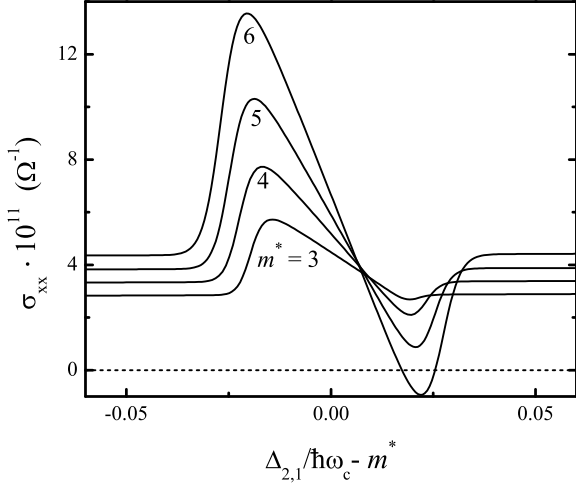


FIG. 7. Evolution of the  $\sigma_{xx}(B)$  line shape near commensurability points with the gradual increase in  $m^*$  at  $T = 0.2$  K and  $f = 79$  GHz.

is induced by the MW resonance absolutely in the same way, as it is for electron scattering at vapor atoms. In the case of liquid  $^3\text{He}$ , electron-rippion scattering dominates at low temperatures  $T \leq 0.2$ , where the half-width of the MW resonance  $\gamma$  is substantially reduced. According to Eq. (37), at the same amplitude of the MW field, this decrease in  $\gamma$  leads to a strong increase in the MW excitation rate  $r$  at the resonance  $\omega = \omega_{2,1}$ , which greatly magnifies  $\nu_A$ .

Unfortunately, the electron-rippion scattering regime is much more difficult for the analysis of the effect of electron heating than the vapor atom scattering regime because of different reasons. First, the electron-rippion coupling  $U_q$  has a very complicated form<sup>11</sup>:

$$U_q(z) = \frac{\Lambda q}{z} \left[ \frac{1}{qz} - K_1(qz) \right] + eE_{\perp} - \frac{\partial V_e^{(0)}}{\partial z_e},$$

where  $K_1(x)$  is the modified Bessel function of the second kind, and  $V_e^{(0)}(z)$  is the electron potential energy over a flat surface. Therefore, it is impossible to obtain simple analytical equations for the energy loss function  $\dot{W}(T_e)$ . Moreover, if  $^3\text{He}$  is used as the liquid substrate, there might be contributions from other mechanisms of energy relaxation, which by now have no strict theoretical descriptions.

As indicated above, heating of SEs only increases the importance of the anomalous contribution to the effective collision frequency. For electron-rippion scattering, it follows directly from Eqs. (25)-(27). Therefore, in order to prove the possibility of existence of zero resistance states due to non-equilibrium filling of the excited subband, it is sufficient to show that negative  $\sigma_{xx}$  can appear even without electron heating. At  $T_e = T = 0.2$  K, the MW field amplitude, which gave  $r = 10^5 \text{ s}^{-1}$  (at  $B = 1$  T)

for the vapor atom scattering regime shown in Fig. 3 (dotted curve), now gives  $r = 2 \cdot 10^6 \text{ s}^{-1}$ , because the MW resonance line width  $2\gamma \simeq 0.3$  GHz due to inhomogeneous broadening<sup>5</sup>. This excitation rate is very high, because it leads to  $\sigma_{xx} < 0$  already at  $m^* = 4$ . For presentation of Fig. 7, we had chosen a two-times lower excitation rate  $r = 10^6 \text{ s}^{-1}$  independent of the magnetic field. This figure shows the evolution of the line shape of conductivity oscillations with the gradual increase in the integer parameter  $m^*$ . It is quite convincing that even without heating of SEs the anomalous contribution to the effective collision frequency increases strongly with  $m^*$ , and the conductivity curve corresponding to  $m^* = 6$  enters the negative conductivity regime in the vicinity of the minimum. This is in accordance with experimental observations reported for the high magnetic field range ( $m^* < 10$ ).

Maxima and minima of  $\nu_A(B)$  have the same amplitude. Without heating of SEs, amplitudes of conductivity maxima obtained here are larger than amplitudes of minima, because the normal contribution  $\nu_N$  increases at  $\Delta_{2,1}/\hbar\omega_c \rightarrow m$  due to oscillations of subband occupancies. Experimental curves<sup>5</sup> show that at strong MW power and large  $m^*$  amplitudes of minima are larger. This could be an indication of electron heating, because  $\nu_N \sim 1/T_e$ . To analyze the effect of heating of SEs on conductivity oscillations, we shall model electron temperature oscillations using similarities in the line shapes of  $T_e - T$  and  $\bar{n}_1 - 1/2$  shown in Fig. 6. In particular, we assume that an electron temperature peak is described by  $T_e(B) = T + 2(\Delta T_e)_{\max} [\bar{n}_1(B, T) - 1/2]$ , where the maximum elevation  $(\Delta T_e)_{\max}$  depends of  $m^*$ . We disregard the asymmetry of the peak induced by  $\dot{W}_A$  because it does not lead to a substantial change in final results. The results of such a model treatment of the heating effect are shown in Fig. 8. They indicate that even moderate heating of SEs affects strongly the shape of magnetooscillations, making amplitudes of minima larger than amplitudes of maxima (dotted curve) in accordance with experimental data.

In Fig. 8, we had chosen the excitation rate  $r = 10^6 \text{ s}^{-1}$ , so that the initial curve (solid) calculated for  $T_e = T$  have a small minima with  $\sigma_{xx} > 0$ . Then, we found that heating with  $(\Delta T)_{\max} = 0.1$  K strongly reduces conductivity extremes due to  $\nu_N \sim 1/T_e$ , and moderate heating with  $(\Delta T)_{\max} = 0.5$  K leads to a minimum with  $\sigma_{xx} < 0$ . Therefore, decay heating of electrons, which occurs in the vicinity of the commensurability conditions, helps to obtain zero resistance states. For example, within the validity range of the two-subband model, electron temperature peaks of about 2 K can reduce  $\nu_N$  by an order of magnitude. Still, heating alone cannot make  $\sigma_{xx} \leq 0$ . It is only the anomalous contribution  $\nu_A$  which eventually leads to negative conductivity and zero-resistance states. Without  $\nu_A$ , a conductivity dip would be an even function of the parameter  $\omega_{2,1} - m^*\omega_c$  with  $\sigma_{xx} > 0$ . The existence of a magnetoconductivity maxima at the opposite side of the point  $\omega_{2,1} - m^*\omega_c = 0$  in

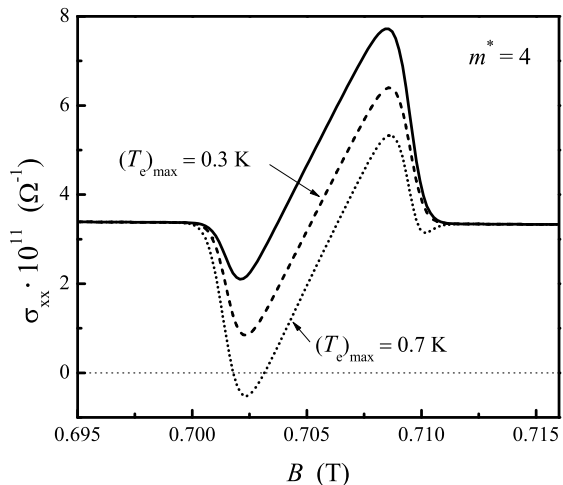


FIG. 8. Evolution of the  $\sigma_{xx}(B)$  line shape near the commensurability point  $m^* = 4$  with the increase in  $(\Delta T_e)_{\max}$  at  $T = 0.2$  K and  $f = 79$  GHz:  $(\Delta T_e)_{\max} = 0$  (solid), 0.1 K (dashed), and 0.5 K (dotted).

experimental curves, which demonstrate vanishing magnetoconductivity<sup>5</sup>, is an additional evidence for a sign-changing correction convincing that ZRS are realized at the vanishing points.

It should be noted that at  $T = 0.2$  K, one-ripplon scattering processes are not sufficient to prevent strong heating of the electron system at the commensurability conditions. In particular, for  $r = 5 \cdot 10^5 \text{ s}^{-1}$ , estimation gives  $(T_e)_{\max} \sim 3$  K at  $m^* = 4$ . The model treatment of the heating effect discussed here allows to draw conclusions about actual role of the electron heating in experiments with SEs<sup>5</sup>. For example, the firm conductivity maximum (without a minima) observed for radiation power  $P$  of -25 dB at  $m^* = 4$  surely indicates that electron heating is small or moderate under these conditions, and there is an additional mechanism of energy relaxation at low ambient temperatures. We speculate, that the magnetopolaronic effect and electron coupling with bulk quasi-particles, giving a very small correction to the momentum relaxation rate under experimental conditions, can contribute substantially to the energy relaxation rate reducing electron temperature.

Experiments<sup>4,5</sup> are conducted for low surface electron densities  $n_s$  of about  $10^6 \text{ cm}^{-2}$ . Nevertheless, electron-electron interaction affects noticeably experimental data. According to Ref. 21, under magnetic field an electron moves in a quasi-uniform electric field of other electrons  $E_f$  of fluctuational origin. Its average value  $E_f^{(0)} \simeq 3\sqrt{T_e}n_s^{3/4}$  increases strongly with electron temperature and density. The fluctuational electric field increases the broadening of the DSF<sup>11,16</sup>  $\Gamma_{l,n;l',n'} \rightarrow \sqrt{\Gamma_{l,n;l',n'}^2 + x_q \Gamma_C^2}$ , where  $\Gamma_C = \sqrt{2}eE_f^{(0)}l_B \propto 1/\sqrt{B}$ . Thus, at  $T_e = 0.2$  K, and  $n_s = 0.9 \cdot 10^6 \text{ cm}^{-2}$ , the Coulom-

bic correction increases  $\Gamma_{l,n;l',n'}$  by about 1.3, if we assume  $x_q \simeq 1$ . If we take into account that the integrand of Eq. (24) has a maximum at  $x_q \sim m^* + 2$ , the broadening increases approximately two times. Therefore, a qualitative analysis indicates that the many-electron effect becomes more important in the low magnetic field range where it increases the width of conductivity oscillations and reduces amplitudes of maxima and minima, which also agrees with experimental observations. Decay heating increases the Coulombic correction to the broadening of magnetooscillations. Still, a strict description of Coulombic effects on magnetoconductivity oscillations requires a more careful study.

## VI. CONCLUSION

In summary, we have developed the theory of magnetoconductivity oscillations in a multi-subband 2D electron system under MW irradiation of a resonant frequency. We have shown that besides the quite obvious  $1/B$ -modulation of conductivity, the non-equilibrium filling of the excited subband induced by the MW resonance leads also to sign-changing corrections to the effective collision frequency due to usual inter-subband scattering. As the MW power goes up, the corresponding increase in the amplitude of these sign-changing corrections can result in the negative linear response conductivity and zero-resistance states.

Our theory is based on the self-consistent Born approximations, and it is presented in a general way applicable for any quasi-elastic scattering mechanism. As particular examples, we have considered two kinds of scatterers which are typical for the electron system formed on the free surface of liquid helium: helium vapor atoms and capillary wave quanta (ripplons). In the vapor atom scattering regime, we found a strong  $1/B$ -modulation of the electron temperature, which increases sharply in the vicinity of commensurability conditions. This decay heating is shown to enhance the effect of the sign-changing terms in the longitudinal conductivity  $\sigma_{xx}$ . The evolution of the line-shape of conductivity oscillations with an increase of the MW field amplitude is studied, taking into account heating of surface electrons.

For the electron-ripplon scattering regime, we have shown that magnetooscillations of large amplitude and the negative linear response conductivity of SEs can easily appear under moderate MW excitation even for cold SEs. The evolution of the line-shape of  $\sigma_{xx}$  extremes caused by an increase in the electron temperature is studied using a model treatment. We believe that theoretical results presented in this work explain all major features of MW-resonance-induced magnetooscillations observed in the system of SEs on liquid helium, and support the suggestion<sup>4,5</sup> that novel zero-resistance states are realized in such a system.

## Appendix A: Energy relaxation rate

Here we give final expressions for the energy relaxation rate of SEs due to scattering with vapor atoms. The normal  $\tilde{\nu}_N^{(a)}$  and anomalous  $\tilde{\nu}_A^{(a)}$  energy relaxation rates are defined by the following relationships:  $\dot{W}_N = -(T_e - T)\tilde{\nu}_N^{(a)}$ , and  $\dot{W}_A = -T\tilde{\nu}_A^{(a)}$ . In turn,  $\tilde{\nu}_N^{(a)} =$

$$\tilde{\nu}_{N,inter}^{(a)} = \frac{\nu_0^{(a)} m_e \hbar \omega_c E_R}{\pi^{1/2} M T_e} \sum_{l>l'} \frac{\bar{n}_l + \bar{n}_{l'} e^{-\Delta_{l,l'}/T_e}}{\Gamma_{l;l'}} \left\{ u_{l,l'} F_{l,l'}(\omega_c) + \frac{\hbar \omega_c}{E_R} p_{l,l'} \left[ F_{l,l'}(\omega_c) \coth\left(\frac{\hbar \omega_c}{2T_e}\right) + H_{l,l'}(\omega_c) \right] \right\}, \quad (\text{A2})$$

functions  $F_{l,l'}$  and  $H_{l,l'}$  were given in Eqs. (40) and (41).

$$\tilde{\nu}_A^{(a)} = \frac{2\nu_0^{(a)} m_e \hbar \omega_c E_R}{\pi^{1/2} M} \sum_{l>l'} \frac{(n_l - n_{l'} e^{-\Delta_{l,l'}/T_e})}{\Gamma_{l;l'}^2} \left\{ u_{l,l'} \Phi_{l,l'}(\omega_c) + \frac{\hbar \omega_c}{E_R} p_{l,l'} \left[ \Phi_{l,l'}(\omega_c) \coth\left(\frac{\hbar \omega_c}{2T_e}\right) + \Theta_{l,l'}(\omega_c) \right] \right\}, \quad (\text{A3})$$

where  $\Phi_{l,l'}$  and  $\Theta_{l,l'}$  are the same as those of Eq. (42). For equilibrium subband occupancies,  $\tilde{\nu}_A = 0$ . These equa-

$\tilde{\nu}_{N,intra}^{(a)} + \tilde{\nu}_{N,inter}^{(a)}$ , where

$$\tilde{\nu}_{N,intra}^{(a)} = \frac{\nu_0^{(a)} m_e \hbar \omega_c E_R}{\pi^{1/2} M T_e} \sum_l \frac{\bar{n}_l}{\Gamma_{l;l}} \times \left[ u_{l,l} + \frac{\hbar \omega_c}{E_R} p_{l,l} \coth\left(\frac{\hbar \omega_c}{2T_e}\right) \right], \quad (\text{A1})$$

The anomalous energy relaxation rate can be represented as

tions were used for obtaining electron temperature as a function of the magnetic field under the MW resonance.

- <sup>1</sup> M.A. Zudov, R.R. Du, J.A. Simmons, and J.R. Reno, Phys. Rev. B **64**, 201311(R) (2001).
- <sup>2</sup> R. Mani, J.H. Smet, K. von Klitzing, V. Narayanamurti, W.B. Johnson, and V. Umansky, Nature **420**, 646 (2002).
- <sup>3</sup> M.A. Zudov, R.R. Du, L.N. Pfeiffer, and K.W. West, Phys. Rev. Lett. **90**, 046807 (2003).
- <sup>4</sup> D. Konstantinov and K. Kono, Phys. Rev. Lett. **103**, 266808 (2009).
- <sup>5</sup> D. Konstantinov and K. Kono, Phys. Rev. Lett. **105**, 226801 (2010).
- <sup>6</sup> A.V. Andreev, I.L. Aleiner, and A.J. Millis, Phys. Rev. Lett., **91**, 056803 (2003).
- <sup>7</sup> V. I. Ryzhii, Fiz. Tverd. Tela **11**, 2577 (1969) [Sov. Phys. Solid State **11**, 2078 (1970)]; V.I. Ryzhii, R.A. Suris, and B. S. Shchamkhalova, Fiz. Tekh. Poluprovodn. **20**, 2078 (1986) [Sov. Phys. Semicond. **20**, 1299 (1986)].
- <sup>8</sup> A.C. Durst, S. Sachdev, N. Read, and S.M. Girvin, Phys. Rev. Lett. **91**, 086803 (2003).
- <sup>9</sup> I.A. Dmitriev, M.G. Vavilov, I.L. Aleiner, A.D. Mirlin, and D.G. Polyakov, Phys. Rev. B **71**, 115316 (2005).
- <sup>10</sup> Yu.P. Monarkha, Fiz. Nizk. Temp. **37**, 108 (2011) [Low Temp. Phys. **37**, 90 (2011)].

- <sup>11</sup> Yu.P. Monarkha and K. Kono, *Two-Dimensional Coulomb Liquids and Solids*, Springer-Verlag, Berlin Heidelberg (2004).
- <sup>12</sup> M. Saitoh and T. Aoki, J. Phys. Soc. Jpn. **44**, 71 (1978).
- <sup>13</sup> T. Ando and Y. Uemura, J. Phys. Soc. Jpn. **36**, 959 (1974).
- <sup>14</sup> R. Kubo, S.J. Miyake, N. Hashitsume, Solid State Phys. **17**, 269 (1965).
- <sup>15</sup> R.R. Gerhardts, Surf. Sci. **58**, 227 (1976).
- <sup>16</sup> Yu.P. Monarkha, E. Teske, and P. Wyder, Phys. Rep. **370**, No. 1, pp. 1-61 (2002).
- <sup>17</sup> Yu.P. Monarkha, S.S. Sokolov, A.V. Smorodin, and N. Stuard, Fiz. Nizk. Temp., **36**, 711 (2010) [Low Temp. Phys. **36**, 565 (2010)].
- <sup>18</sup> Yu.P. Monarkha, D. Konstantinov, and K. Kono, J. Phys. Soc. Jpn. **76**, 124702 (2007).
- <sup>19</sup> T. Ando, J. Phys. Soc. Jpn. **44**, 765 (1978).
- <sup>20</sup> D. Konstantinov, H. Isshiki, H. Akimoto, K. Shirahama, Yu. Monarkha, and K. Kono, J. Phys. Soc. Jpn. **77**, 034705 (2008).
- <sup>21</sup> M.I. Dykman and L.S. Khazan, Zh. Eksp. Teor. Fiz. **77**, 1488 (1979) [Sov. Phys. JETP **50**, 747 (1979)].